Int. J. Electrochem. Sci., 14 **(2019)** 441 – 452, doi: 10.20964/2019.01.62

International Journal of
ELECTROCHEMICAL
SCIENCE
www.electrochemsci.org

Effect of Electrode Potential on the Drag Force on Gold and Polyvinyl Butyral Surfaces in a Flowing Aqueous Fluoride Solution

Filipas Ambrulevicius, Arunas Pulmanas, Deivis Plausinaitis, Vytautas Daujotis[*]

Institute of Chemistry, Vilnius University, 24 Naugarduko St, LT-03225 Vilnius, Lithuania
[*]E-mail: vytautas.daujotis@chf.vu.lt

Received: 13 April 2018 / *Accepted:* 8 May 2018 / *Published:* 30 November 2018

It is shown that positive electrical polarization reduces the drag force on gold- and polyvinyl butyral (PVB)-coated spheres immersed in a stream of aqueous sodium fluoride solution. This effect is related to a decrease in the interfacial viscosity of the solution at the positively polarized gold and PVB surfaces, as obtained from quartz resonator measurements. The decrease in viscosity at a polymer-coated electrode is larger than that at a gold electrode, which is consistent with drag force measurements. The drag force reduction due to decreased interfacial viscosity at a polymer-coated metallic surface on application of an electrical potential widens the range of possible applications of this effect for active manipulation of wall-bounded liquid flows, given that the use of metal surfaces is limited by their risk of corrosion.

Keywords: Drag force, Gold surface, Polyvinyl butyral surface, Interfacial viscosity, Quartz resonator

1. INTRODUCTION

In wall-bounded flows, small changes in interfacial properties such as viscosity and density may have crucial effects on the fluid flow field. The near-wall viscosity in a liquid boundary layer affects the stability of the wall-bounded flow. Lowering this viscosity makes the normal velocity profile less inflectional, which minimizes the linear growth of unstable waves in boundary layers [1]. Our drag force measurements have shown a reduction in drag force on a gold-coated sphere in flows of hexafluorophosphate, perchlorate, and chloride aqueous solutions during polarization of gold-coated sphere surfaces toward the potential of zero charge, where a minimum in the drag force is observed [2, 3]. The interfacial viscosity, determined using the quartz resonator technique, shows the same trend of change with potential. Furthermore, the shifts in the potential of the minimum values of the drag force and of the interfacial viscosity follow the shift in the potential of zero charge with changing anion

concentrations, and the Esin–Markov relation holds at these potentials [3]. Our findings show that by controlling the applied potential, it should be possible to control the viscosity of the liquid layer close to the solid interface, which enhances the ability to actively manipulate a wall-bounded liquid flow field to effect desired changes.

However, the high cost of gold limits the technological application of this effect. To investigate the possibility of using stainless steel instead of gold, we have measured the drag force on a stainless steel sphere immersed in an aqueous sulfate or chloride solution stream, but have not found any pronounced trend in the dependence of the drag force on an applied potential. The presence of certain anions adsorbed on the surface or incorporated into the passive film on stainless steel is detrimental to film stability and leads to pit initiation [4]. The resistance of stainless steel to corrosive attack decreases still further when an anodic potential is applied. In addition, because stainless steel is an alloy, its surface composition is subject to changes when a potential is applied. Thus, it seems that stainless steel is not a viable alternative to gold in this context. A more promising approach appears to be the use of polymer-coated surfaces. Analysis of the admittance of a quartz resonator in contact with an aqueous solution has shown that the viscosity–density product of water at a styrene–butadiene-coated electrode surface decreases during a positive potential scan [5].

The purpose of the present work is to study and compare the effect of electrode potential on the drag force on gold-coated and polymer (polyvinyl butyral resin, PVB)-coated spheres using two different techniques: (i) measurement of the drag force on a sphere immersed in a stream of aqueous solution; (ii) evaluation of the effect of electrode potential on the properties of a solution layer at gold and PVB surfaces by studying (a) the high-frequency admittance behavior of quartz-resonator-supported electrodes and (b) the frequency behavior of a dual-quartz resonator (two resonators with differently textured electrode surfaces in a monolithic sensor).

2. EXPERIMENTAL

Measurement and analysis of electrode potential effect upon the drag force on gold-coated and PVB-coated spheres immersed in a stream of aqueous solution has been performed by using experimental set-up. Its structure and functioning have been described in detail previously [2, 3, 6]. The sphere was located in the centre of the vertically positioned bronze tube of inner diameter 4.3 cm and 40 cm long and 1.5 cm below the upper reservoir bottom were nearly inviscid aqueous solution converges and enters the tube. The spheres used were steel balls of diameter 9.52 mm from bearings. The ball was attached to a gold wire of diameter 0.1 mm by arc welding. The wire served for hanging the immersed ball on the weighing hook of an analytical balance (measures drag force) and for connecting potentiostat to the ball (working electrode). The vertical bronze tube was used as counter electrode.

For measurements at gold surface, the ball was electrochemically coated with thin copper underlayer and gold (0.01 mm thick) before attaching gold wire. For measurements at a PVB surface, the ball with attached wire was dip-coated with PVB. This dip-coating, with subsequent evaporation of volatiles, was repeated three times. The thickness of the final PVB layer was 6 μm. For dip-coating, a

3.5% solution of PVB (Butvar B-90, Eastman Chemical) was prepared in a combination of 60 parts toluene and 40 parts ethanol (95%) by weight.

Non-parametric regression method LOESS (LOcal smoothing technique with tri-cube weighting and polynomial regrESSion) [7] was used to smooth the drag force data as a function of the potential.

Properties of solution layers at electrically polarized surfaces were investigated using piezoelectric resonator techniques. Viscosity and density values were calculated from frequency shifts occurring upon immersion of a gold-coated dual-quartz resonator (two resonators with differently textured surfaces in a monolithic sensor) into a solution. The setup for measuring the potential dependences of frequency shifts and their analysis have been described previously [2].

For measuring solution properties at a PVB surface, the quartz resonator admittance technique was used. Admittance measurements and analysis of admittance data according to the modified Butterworth–Van Dyke equivalent circuit were performed as described previously [2, 5]. For the resonators, 5-MHz AT-cut quartz crystals of diameter 15 mm and thickness 0.33 mm (Valpey Fisher) were used. Each resonator was constructed by vacuum coating of centered circular areas (9.6 mm diameter) of both sides of a crystal with a titanium underlayer (10 nm thick) and gold (200 nm thick). For measurements at PVB surfaces, one surface of the resonator was spin-coated with PVB (4 μm thick). For spin-coating, the same solution as for dip-coating was used. In order to verify the suitability of PVB coated resonator for measuring solution properties, the roughness of PVB surface was analyzed by using Veeco Nanoscope IV Multimode AFM.

Potentials were measured against a silver/silver chloride/(saturated KCl) reference electrode (Ag/AgCl).

The PVB resin used for electrode surface coating was again Butvar B-90. Sodium fluoride (99%, Sigma-Aldrich) was used to prepare the solutions. For the piezoelectric resonator experiments and the drag force measurements, doubly distilled water and singly distilled (after deionization) water were used, respectively.

3. RESULTS AND DISCUSSION

3.1. Measurement of effect of electrode potential on drag forces on gold- and PVB-coated spheres in aqueous fluoride solution

Drag forces on gold- and PVB-coated spheres were measured in the potential regions from −100 to +500 mV and from 0 to +500 mV, respectively. The sampling rate for both drag force and flow velocity was 5 per second. The drag coefficients C_D for the spheres were calculated from the recorded drag force F_D via the expression [8]

$$C_D = \frac{8F_D}{\pi\rho v_\infty^2 d^2}, \quad (1)$$

where ρ, v_∞, and d are the density of the fluid, the unbounded flow velocity, and the sphere diameter, respectively. v_∞ was obtained by correcting the measured average flow velocity for the wall effect. As there is no general theory of sphere drag, this correction was accomplished using empirical

relationship between drag coefficient C_D and Reynolds number *Re*. In this work, the average flow velocity was around 0.18 m/s. Then the Reynolds number for the sphere (diameter d = 9.52 mm) immersed in this aqueous solution flow is $Re = \rho v_\infty d/\eta \approx 1700$. This value is in the Reynolds number range from 1.5×10^3 to 1.2×10^4, for which Clift et al. [9] have proposed empirical relationship

$$\lg C_D = -2.4751 + 2.5558w - 0.9295w^2 + 0.1049w^3, \quad (2)$$

where $w = \lg Re$. Equations (1) and (2) and the expression for the Reynolds number were used in an iterative procedure to correct the measured average flow velocity for the wall effect and to obtain v_∞. For a gold-coated sphere, this was found to be equal to 0.2064 m s^{-1}, whereas the measured average flow velocity was 0.1806 m s^{-1}. For a PVB-coated sphere, the unbounded and measured average flow velocities were 0.1755 and 0.17423 m s^{-1}, respectively.

A nonparametric regression analysis was applied to reveal any possible dependence of the drag coefficient on the potential, as described previously [2, 3]. Figures 1(a) and 2(a) (solid lines) show LOESS fits with a sampling proportion of 0.3 for gold-coated and PVB-coated sphere drag, respectively, versus potential.

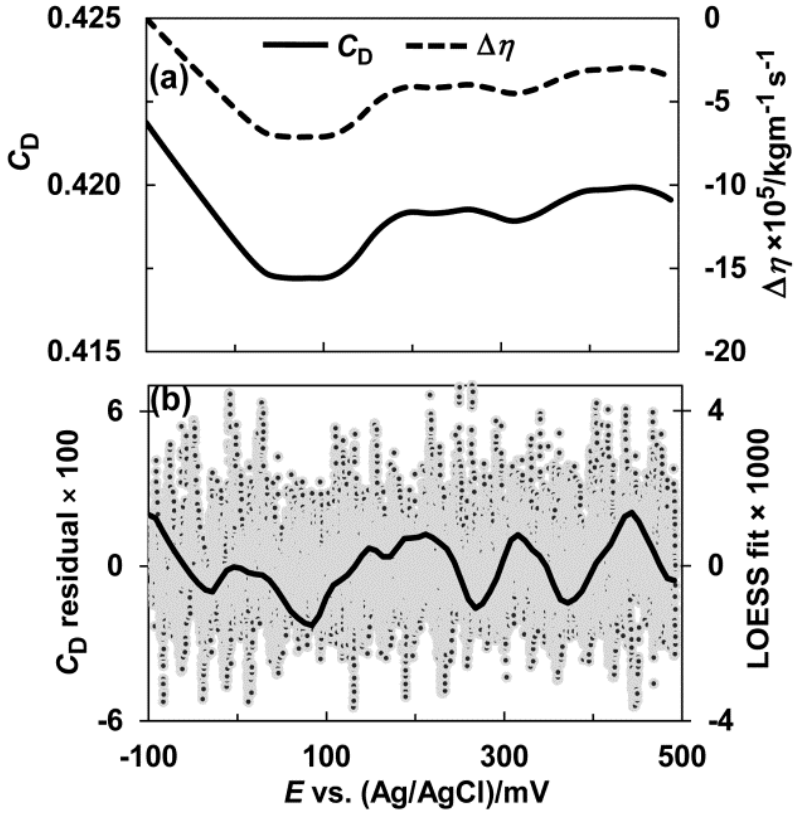

Figure 1. Drag force data on solution-layer properties at a gold-coated sphere. (a) LOESS fit for gold-coated sphere drag (solid line; the sampling proportion and polynomial degree are 0.3 and 1, respectively) and calculated apparent viscosity change (dashed line) versus potential of gold electrode in 0.1 M NaF aqueous solution; two potential cycles, dE/dt = 0.5 mV s^{-1} (20280 drag force coefficients), v_∞ = 0.2064 m s^{-1}, temperature from 21.1°C to 21.3°C. (b) Scatter plot (dots) of drag coefficient residuals [LOESS fit in Fig 1(a)] and their LOESS fit (solid line; sampling proportion and polynomial degree are 0.15 and 1, respectively) versus potential.

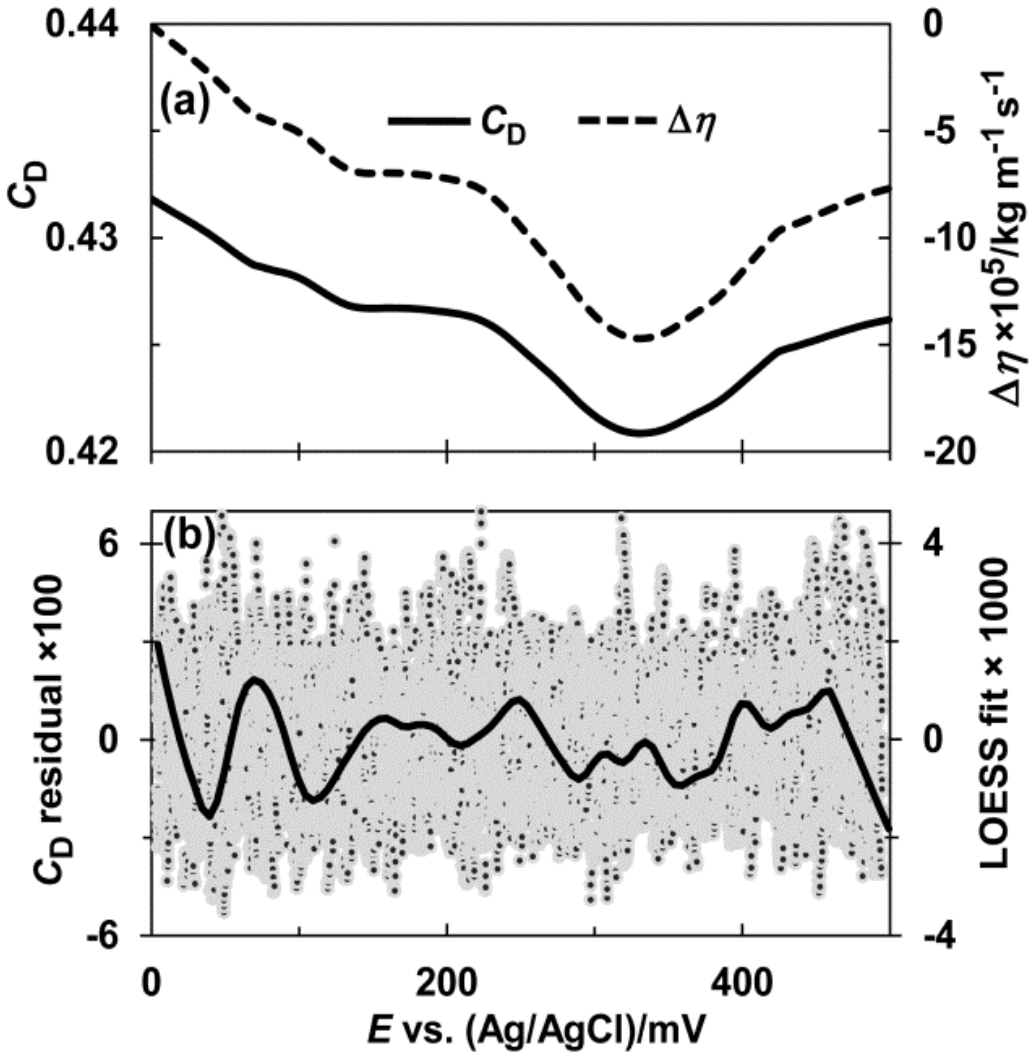

Figure 2. Drag force data on solution-layer properties at a PVB-coated sphere. (a) LOESS fit for PVB-coated sphere drag (solid line; sampling proportion and polynomial degree are 0.3 and 1, respectively) and calculated apparent viscosity change (dashed line) versus potential of PVB-coated electrode in 0.1 M NaF aqueous solution; five potential cycles, dE/dt = 1.0 mV s^{-1} (24840 drag force coefficients), v_∞= 0.1755 m s^{-1}, temperature from 21.6°C to 21.9°C. (b) Scatter plot (dots) of drag coefficient residuals [LOESS fit in Fig. 2(a)] and their LOESS fit (solid line; sampling proportion and polynomial degree are 0.15 and 1, respectively) versus potential.

As LOESS fit lines are not regression-based, the goodness of this fit was evaluated by plotting its residuals versus potential [dots in Figs. 1(b) and 2(b)] and again applying the LOESS smoothing technique to smooth the drag coefficient residuals as a function of potential [solid curves in Figs. 1(b) and 2(b)]. Although the smaller sampling proportion used (0.15) highlights the trends in residuals, these do not affect the main features of the LOESS fits presented as solid lines in Figs. 1(a) and 3(a).

Figures 1(a) and 2(a) show that the switch from a gold to a PVB surface shifts the minimum position of C_D and interfacial viscosity from +70 to +330 mV.

Figures 1(a) and 2(a) show the changes of apparent viscosity with potential (dashed lines), which were calculated from C_D via Eq. (2) and the expression for *Re*. The calculated viscosity is

termed as apparent, because the result of this calculation is a very rough estimate. The reason was discussed in our previous paper [6]. Drag forces on a sphere arise primarily from viscous shear stresses (skin friction) and differences in pressure, which are interdependent [10]. The use of the empirical relationship (2) to calculate viscosity changes is based on the assumption that changes in the drag force are attributable only to changes in skin friction and that the possible changes in pressure differences are neglected. Therefore, interfacial viscosity changes calculated in this way should be considered only as approximations. They are presented here just for comparison with interfacial viscosity data obtained using the quartz resonator technique and presented in the next section.

3.2. Quartz resonator measurements of the effect of electrode potential on the viscosity of aqueous fluoride solutions at gold- and PVB-coated electrode surfaces

Positive potential scans of nontextured and textured resonators were performed simultaneously and repeated three times in the same 0.1 M NaF solution. Resonant frequencies of nontextured and textured resonators (f_N and f_T, respectively) were recorded at 12-mV increments starting from the open-circuit potential. The value of the resonant frequency measured before immersion was subtracted from each recorded frequency value. The measured resonant frequency shifts Δf_N and Δf_T were transformed into viscosity η and density ρ values using the semi-empirical equations [11]

$$\Delta f_N = -c_{11}(\rho\eta)^{-1/2} - c_{12}\rho, \quad (3)$$

$$\Delta f_T = -c_{21}(\rho\eta)^{-1/2} - c_{22}\rho, \quad (4)$$

where the coefficients c_{ij} were determined in advance from Δf_N and Δf_T measured upon immersion into different liquids of known viscosity and density. These measurements and those in fluoride solutions were performed in one series of experiments using an unchanged experimental setup, which was also used for measurements in hexafluorophosphate, chloride, and perchlorate solutions [2, 3]. In this series, the coefficients were determined as

$$c_{11} = 632.5\ \mathrm{kg^{-1}m^2s^{-1/2}}, \qquad c_{12} = 0.671\ \mathrm{kg^{-1}m^3s^{-1}},$$

$$c_{21} = 742.5\ \mathrm{kg^{-1}m^2s^{-1/2}}, \qquad c_{22} = 3.528\ \mathrm{kg^{-1}m^3s^{-1}}.$$

The changes in $\rho\eta$ and η with potential are shown in Fig. 3. The minimum values of $\rho\eta$ and η are observed at approximately −160 mV. Quartz resonator admittance measurements, which allow separation of the effects of changes in electrode mass due to adsorption of solution species, gave a similar change in $\rho\eta$, but the position of the minimum was slightly less negative (approximately −120 mV).

The changes in the product of interfacial viscosity and density with potential shown in Fig. 3(a) are presented for comparison with the data shown in Fig. 5. It should be noted that, compared with the viscosity change in Fig. 3(b), the density change is much less and does not exceed 0.1% of the bulk value.

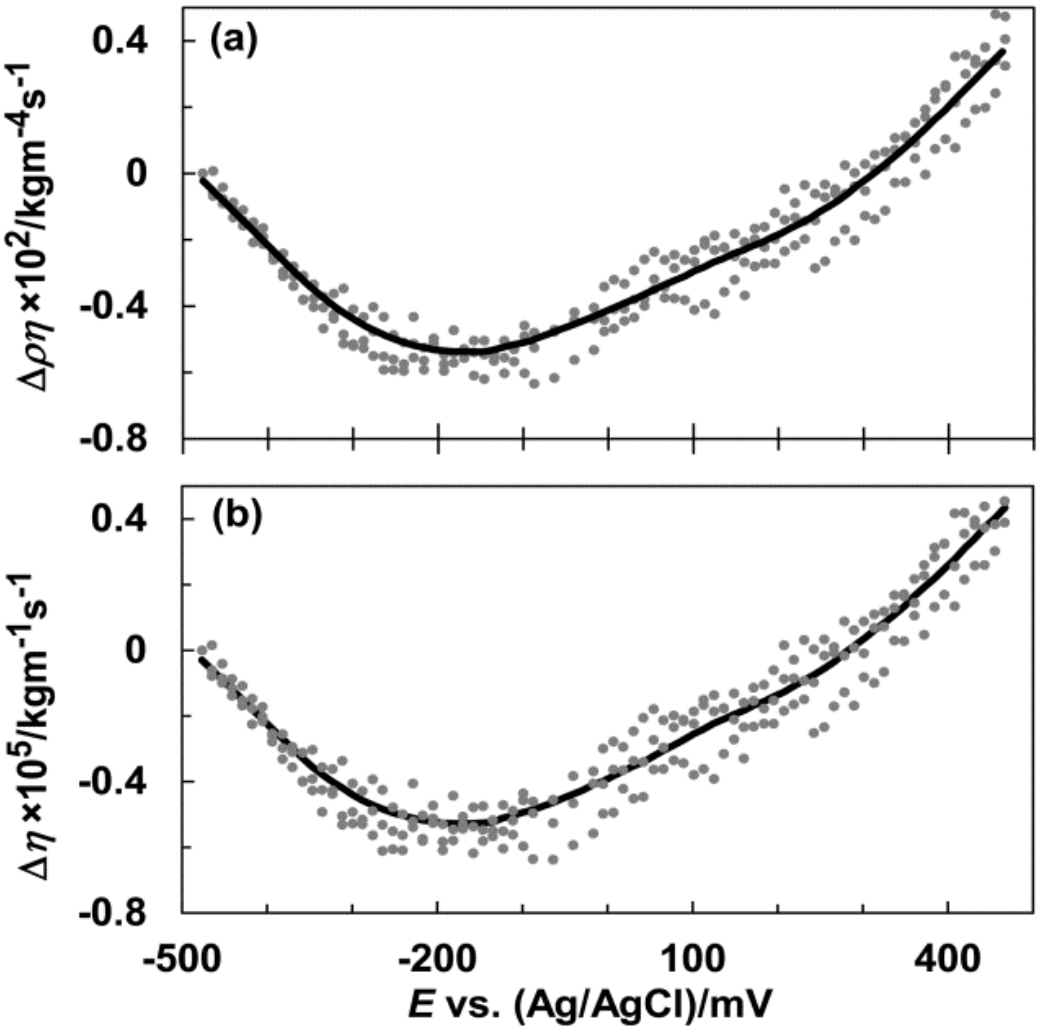

Figure 3. Changes in (a) the smoothed product of interfacial viscosity and density and (b) the smoothed interfacial viscosity, together with their scatter plots (dots from three potential scans in the positive direction) versus potential of gold electrode in 0.1 M NaF aqueous solution; dE/dt = 100 mV s^{-1}, T = 22.2±0.02°C.

The dual-quartz resonator with differently textured PVB surfaces was not used for investigation of solution-layer properties at a PVB-coated electrode surface. It is rather complicated to ensure a uniform thickness of the PVB film over the whole resonator surface, which is specially corrugated in advance. In addition, the potential distribution on such a surface would be ill-defined. For these reasons, the quartz resonator admittance technique was used, even though it does not allow separate determination of the liquid viscosity and density, but only of their product.

Before and after quartz resonator admittance measurements, the characteristics of the PVB coating deposited on the quartz resonator were assessed using electrochemical impedance spectroscopy (EIS). Bode plots for a PVB-coated quartz-supported gold electrode exposed to 0.1 M NaF solution show that the ac impedance value measured at 0.1 Hz does not noticeably change during admittance measurements, remaining at about $10^8\ \Omega\ \mathrm{cm}^{-2}$, which allows us to conclude that a PVB coating

provides good protection for coated metal surface and does not degrade during admittance measurements [12].

In the present work, admittance data were analyzed according to a model assuming a smooth resonator surface. According to Urbakh et al. [13], this approximation can be justified if the surface has only a very slight roughness, with $h/l \ll 1$ (where *h* is the average roughness height and *l* is the average lateral distance between roughness peaks) and with a roughness less than 10 nm, since the impedance of the quartz resonator would be expected to respond to roughness above this height. An atomic force microscope (AFM) image and the corresponding cross-sectional contour (Fig. 4) show the typical roughness characteristics of the PVB-coated surfaces used in the present work for admittance measurements. A roughness analysis of 4 μm^2 of the gold surface shown in Fig. 4 gives a maximum vertical distance between the highest and lowest data points in the AFM image of 2.43 nm and a root-mean-square average deviation from the mean data plane of 0.48 nm. These data and the cross-sectional contour in Fig. 4 justify the use of the simplified model (a resonator with an ideally smooth surface) for the admittance data analysis.

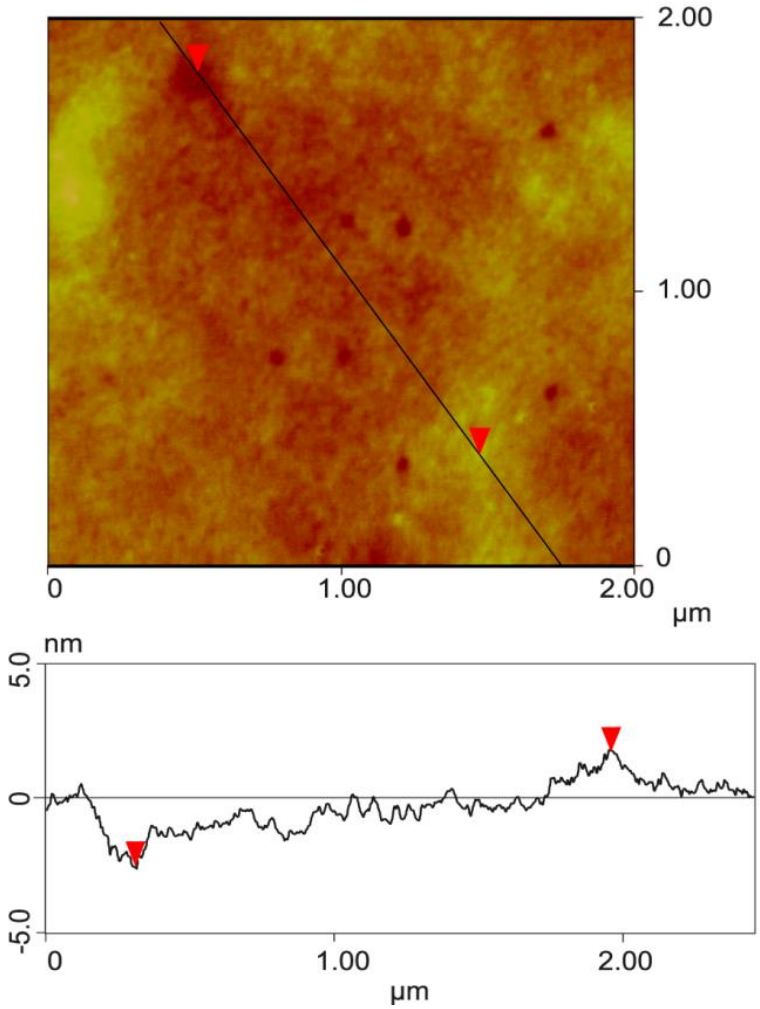

Figure 4. AFM image and corresponding cross-sectional contour of a surface of PVB coating deposited on a resonator electrode.

For one potential scan from −200 to +750 mV, frequency spectra of admittance magnitude and phase angle were measured in 25-mV steps. At each potential step, frequency spectra (150 frequency values, 25 Hz apart) of admittance magnitude and phase angle were measured during about 13 s. Full potential scan measurements were performed during approximately 9 min. Analysis of the measured admittance data was performed according to the modified Butterworth–Van-Dyke equivalent circuit for an AT-cut quartz resonator with contributions from the mass of the rigid film and from the viscosity and density of the liquid in contact with one face of the quartz resonator. The obtained values of circuit elements were transformed into the product of the dynamic viscosity and density of the solution layer adjacent to the electrode surface as described earlier [5]. The changes in this product with potential are shown in Fig. 5.

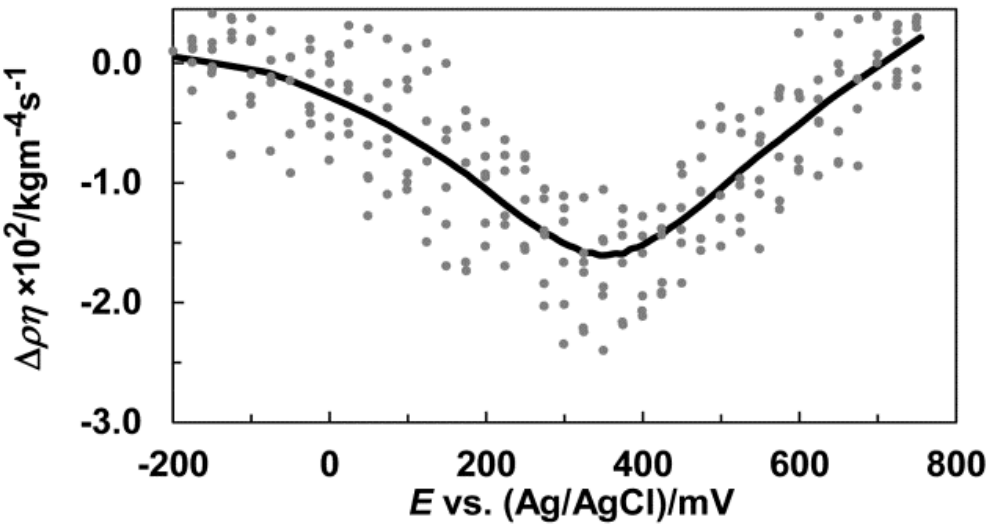

Figure 5. Changes in smoothed product of interfacial viscosity and density (solid line) and its scatter plot (dots from six potential scans in the positive direction) versus potential of a PVB-coated gold electrode in 0.1 M NaF aqueous solution; t = 22.5±0.05°C.

At the beginning of this section, an AFM analysis of the roughness of the surface of the PVB-coated resonator electrode was presented with the aim of assessing the suitability of the resonator used for measuring liquid properties. Cho et al. [14] have shown that quartz resonator admittance data themselves can be used for such an assessment. They proposed a so-called signature S_2, which can be used as an indicator of correct instrument measurement under liquid loading conditions:

$$S_2 = \frac{|\Delta f|}{N\Delta D} = f_U/2, \quad (5)$$

where Δf and ΔD are the changes in resonant frequency and dissipation that occur upon immersion of the quartz resonator into liquid, N is the harmonic number, and f_U is the fundamental resonant frequency of the unloaded resonator. The theoretical value of S_2, equal to one-half the fundamental resonant frequency, is obtained when the recorded data do not reflect artifacts such as coupling of surface roughness to the loading liquid. When S_2 is calculated from the values of the Butterworth–van Dyke equivalent circuit components, obtained from circuit admittance analysis, deviations less than 10% are acceptable for proper operation of the instrument [14]. In our

measurements, S_2 was found to be 2.751×10^6 Hz, which deviates from 2.493×10^6 Hz (one-half the fundamental resonant frequency of the resonator used) by approximately 10%. Thus, this result is in accord with the data from AFM surface roughness analysis and serves as additional evidence of proper resonator operation.

A comparison of the changes in interfacial solution properties at gold- and PVB-coated electrodes (Figs. 3 and 5) reveals that the potential effect is several times stronger in the case of polymer-coated electrodes. At a PVB surface, the minimum of the product of viscosity and density is approximately three times deeper. The same ratio holds for the changes in apparent viscosity calculated from drag force data [the dashed lines in Figs. 1(a) and 2(a)], although their absolute magnitudes are almost ten times larger.

From the quartz resonator data on solution properties, it is reasonable to conclude that the reduction in drag force is due primarily to a decrease in interfacial viscosity caused by the applied potential. Switching from a gold to a PVB surface shifts the drag force minimum toward more positive potentials, which is also the case for the interfacial viscosity. Moreover, at a PVB surface, the minimum value of the product of viscosity and density is observed at +330 mV (Fig. 5), which corresponds to the minimum drag force on a PVB-coated sphere [Fig. 2(a)]. At a gold surface, the difference in the positions of the minima [Figs. 1(a) and 3] is probably due to the different structures of the vacuum-deposited (resonator) and electrodeposited (steel ball) gold layers. An electrodeposited gold layer is usually characterized by some degree of porosity and may contain inclusions from the plating solution, which will affect the surface charge and the double-layer capacitance. These electrode properties can have a crucial impact on the viscosity of the solution layer adjacent to the electrode surface [2, 3]. This explanation is in accord with the fact that the position of the minimum coincides with that for a PVB-coated surface [cf. Figs. 2(a) and 5]. The agreement between the positions of the minima is to be expected, since the surfaces of the PVB coatings in the two cases should not differ to any great extent, both having been obtained from the same PVB solution.

Using electrochemical AFM, Guriyanova et al. [15] have shown that the viscosity of a liquid layer close to a solid interface can be controlled by adjusting the applied potential. They explain the decrease in viscosity in terms of decreasing surface charge and electric field at the surface when the applied potential is shifted toward the potential of zero charge. Our earlier findings [2, 3] and the change in interfacial viscosity at a gold electrode in fluoride solution seen in Fig. 3(b) are in accord with this explanation.

A probable explanation for the effect of the potential on the viscosity of water at a PVB-coated electrode surface can be related both to changes in surface charge and to changes in surface hydrogen bonding conditions due to altered alignment of PVB functional groups. In Butvar B-90, the contents of hydroxyl, acetate, and butyral expressed as percentages of the corresponding acetals are 18.0–20.0%, 0–2.5%, and 80%, respectively. The application of a potential to a PVB-coated electrode may lead to a persistent electrical polarization in the PVB film resulting from alignment of dipoles and to migration of charge carriers over macroscopic distances, with subsequent accumulation near the electrode surface. Investigations of thermally stimulated depolarization (TSD) currents in PVB films [16,17] have led to the conclusion that a depolarization current appears owing to disorientation of aligned dipoles involving the acetate and hydroxyl side and end groups. It has also been shown that motions of

large parts of the main chain cannot be excluded [18]. A TSD study of films of polyvinyl acetate, which differs from PVB by the absence of butyral groups, has shown that adsorbed water forms clusters of water complexes, thereby increasing the activation energy of depolarization [19]. Potential polarization can lead to disorder in the extended network of interfacial water molecules. This can shift the equilibrium in the direction of smaller water clusters and make the layer near the PVB surface less viscous.

4. CONCLUSIONS

Drag force and quartz resonator measurements have shown that the reduction in the drag force on a sphere that is observed in the case of positive electrical polarization of the sphere surface is related primarily to a decrease in the interfacial solution viscosity. The effects of electrode potential on the interfacial viscosity of a 0.1 M NaF aqueous solution layer at a PVB-coated electrode is several times stronger than at a gold electrode surface. The minimum values of the drag force and the interfacial viscosity at a PVB electrode are shifted toward more positive potentials. In quartz resonator measurements, the greatest decreases in interfacial viscosity at gold and PVB surfaces were found to be about 0.6% and 1.5% of the bulk viscosity, respectively. Drag force measurements gave the same relative decreases, but the calculated absolute magnitudes of the decreases in apparent viscosity were almost an order of magnitude greater than those obtained from the quartz resonator measurements. This result is in accord with the results obtained for all solutions studied previously [2, 3].

There can be several reasons for the discrepancy between the values of the interfacial viscosity determined from drag force and quartz resonator measurements. First, viscosity is a continuum property, and the interfacial viscosity, if it changes with distance from the interface, can only be determined by averaging along that distance when non-probe-based methods are used. Different sensors usually average over different distances from the surface. Piezoelectric resonator measurements determine the interfacial viscosity by averaging over the velocity decay lengthscale of damped shear waves radiated from the resonator into the liquid. As there is no quantitative theory of sphere drag in turbulent flow, the thickness of the layer, the average viscosity of which is determined in drag force measurements, is poorly defined. Second, the drag forces on a sphere arise primarily from viscous shear stresses (skin friction) and differences in pressure, which are interdependent. Calculation of changes in viscosity via the empirical relationship (2) rely upon the assumption that changes in drag force are attributable mainly to changes in skin friction, and they neglect the dependence on pressure differences. This could lead to overestimation of the viscosity when pressure effects favor drag reduction.

The present work shows that by controlling the potential applied to a polymer-coated metal interface, it is possible to actively manipulate wall-bounded liquid flows. This may widen the range of possible technological applications of this effect, given that the use of metal surfaces is limited owing to the increased risk of corrosion of such surfaces when the electrode potential is shifted toward more positive values.

References

1. M. Gad-el-Hak, *Flow Control: Passive, Active, and Reactive Flow Management*, Cambridge University Press (2006) New York.
2. D. Plausinaitis, A. Pulmanas, M. Waskaas, R. Raudonis and V. Daujotis, *Electrochim. Acta.*, 109 (2013) 756
3. D. Plausinaitis, A. Pulmanas, V. Kubilius, R. Raudonis and V. Daujotis, *Electrochim. Acta*, 121 (2014) 278.
4. C.-O. A. Olsson and D. Landolt, *Electrochim. Acta*, 48 (2003) 1093.
5. D. Plausinaitis, M. Waskaas, R. Raudonis, and V. Daujotis, *Electrochim. Acta*, 51 (2006) 6152.
6. A. Pulmanas, D. Plausinaitis, V. Daujotis, *Int. J. Electrochem. Sci*., 10 (2015) 1742.
7. W. S. Cleveland and S. J. Devlin, *J. Amer. Statist. Assoc.*, 83 (1988) 596.
8. N. White, *Fluid Mechanics*, 4th ed., McGraw–Hill (2002) New York.
9. R. Clift, J. R. Grace and M. E. Weber, *Bubbles, Drops and Particles*, Academic Press (1978) New York.
10. H. Schlichting, *Boundary-Layer Theory*, 7th ed., McGraw-Hill (1979) New York.
11. J. Martin, G. C. Frye, and K. O. Wessendorf, *Sens. Actuators* A, 44 (1994) 209.
12. M. McIntyre and H. Q. Pham, *Prog. Org. Coat*., 27 (1996) 201.
13. M. Urbakh, V. Tsionsky, E. Gileadi and L. Daikhin, *Probing the solid/liquid interface with the quartz crystal microbalance*, in C. Steinem, A. Janshoff (Eds.) *Piezoelectric Sensors*, Springer Series on Chemical Sensors and Biosensors, Part I, vol. 5, Springer, Berlin (2007) 111.
14. N.-J. Cho, J. N. D'Amour, J. Stalgren, W. Knoll, K. Kanazawa and C. W. Frank, *J. Colloid Interface Sci.*, 315, (2007) 248.
15. S. Guriyanova, V. G. Mairanovsky, *E. Bonaccurso, J. Colloid Interface Sci*., 360 (2011) 800.
16. K. Jain, N. Kumar and P. C. Mehendru, *J. Electrochem*. Soc,. 126, (1979) 1958.
17. P. C. Mehendru, K. Jain and N. Kumar, *Thin Solid Films*, 70 (1980) 7.
18. J. L. Gil-Zambrano, C. Juhasz, *J. Phys. D: Appl. Phys*., 14 (1981) 1661.
19. P. C. Mehendru, K. Jain and P. Mehendru, *J. Phys. D: Appl. Phys*., 10 (1977) 729.

© 2019 The Authors. Published by ESG (www.electrochemsci.org). This article is an open access article distributed under the terms and conditions of the Creative Commons Attribution license (http://creativecommons.org/licenses/by/4.0/).